Finite fracture mechanics: A coupled stress and energy failure criterion

Pietro Cornetti [a,*], Nicola Pugno [a], Alberto Carpinteri [a], David Taylor [b]

[a] *Dipartimento di Ingegneria Strutturale e Geotecnica, Politecnico di Torino, Corso Duca degli Abruzzi 24, 10129 Torino, Italy*
[b] *Department of Mechanical Engineering, Trinity College, Dublin 2, Ireland*

Abstract

The aim of the present paper is to introduce a new failure criterion in the framework of Finite Fracture Mechanics. Criteria assuming that failure of quasi-brittle materials is affected by stress or energy flux acting on a finite distance in front of the crack tip are widely used inside the scientific community. Generally, this distance is assumed to be small compared to a characteristic size of the structure, i.e. to any length describing the macroscale. A key point of the present paper is to analyse what happens if the smallness assumption does not hold true. The proposed approach relies on the assumption that the finite distance is not a material constant but a structural parameter. Its value is determined by a condition of consistency of both energetic and stress approaches. The model is general. In order to check its soundness, an application to the strength prediction for three point bending tests of various relative crack depths and of different sizes is performed. It is seen that, for the un-notched specimens, the present model predicts the same trend as the Multi-Fractal Scaling Law (MFSL). Finally, a comparison with experimental data available in the literature on high strength concrete three point bending specimens is performed, showing an excellent agreement. It is remarkable to observe that the method presented herein is able to provide the fracture toughness using test data from un-notched specimens, as long as the range of specimen sizes is broad enough.
© 2006 Elsevier Ltd. All rights reserved.

Keywords: Finite fracture mechanics; Fracture toughness; Tensile strength; Size effects

1. Introduction

When dealing with brittle or quasi-brittle materials, two main failure criteria are generally taken into account. The former is a stress criterion:

$$\sigma = \sigma_u \tag{1}$$

---

* Corresponding author. Tel.: +39 0115644901; fax: +39 0115644899.
  E-mail address: pietro.cornetti@polito.it (P. Cornetti).

Nomenclature

(x, y)	space coordinates
σ	generic normal stress (in Section 4: maximum stress in a TPB specimen)
σ_y	normal stress in the y-direction
σ_u	tensile strength
$\mathscr{G}$	crack driving force
$\mathscr{G}_F$	fracture energy
K_I	stress-intensity factor under mode I conditions
K_{Ic}	fracture toughness
a	crack length
Δ_S, Δ_E, Δ_{SE}	finite crack extensions according to stress (S), energy (E) and coupled (SE) approaches
c	dimensionless coefficient in the expression of Δ_E
t	dummy variable
b, d	TPB specimen height and thickness
$\alpha = a/b$	relative crack depth of the TPB specimen
$\varepsilon = \Delta_{SE}/b$	ratio between the finite crack extension and the specimen height
$S_0(x/b)$, $S_\alpha(x/b)$	dimensionless stress function along the ligament, respectively for un-notched specimens and notched specimens with relative crack depth α
$F(a/b)$	shape function in the expression of the SIF for TPB specimens
σ_f	apparent tensile strength of a TPB specimen
$\beta = b/\Delta_S$	dimensionless structural size
$\delta = \Delta_{SE}/\Delta_S$	dimensionless finite crack extension for the coupled (SE) criterion
l_{ch}	material characteristic length in the MFSL expression
σ_0, b_0	strength for a vanishing size and transitional size in the SEL expression

i.e. failure takes place if, at least in one point, the stress σ reaches the *tensile strength* σ_u. The latter is an energetic criterion:

$$\mathscr{G} = \mathscr{G}_F \qquad (2)$$

It states that failure happens if the crack driving force $\mathscr{G}$ equals the crack resistance $\mathscr{G}_F$. $\mathscr{G}_F$ is the so-called *fracture energy*, i.e. the energy necessary to create the unit fracture surface. As is well known, according to Irwin's relationship, the energetic criterion can be expressed equivalently in terms of stress-intensity factor (SIF) K_I and *fracture toughness* K_{Ic}:

$$K_I = K_{Ic} \qquad (3)$$

For the sake of simplicity, only mode *I* crack propagation will be dealt with in the following.

The stress criterion provides good results for crack-free bodies, whereas the energetic criterion is physically sound for bodies containing a sufficiently large crack. Otherwise both the criteria fail. In fact, the stress criterion provides a null failure load for a body containing a crack, the stress field being singular in front of the crack tip. On the other hand, the energetic criterion provides an infinite failure load for a crack-free body, the stress-intensity factor being zero in absence of a crack.

The above mentioned criteria therefore work for the extreme cases (i.e. no crack or large crack) but are no longer valid for the intermediate cases, such as, for instance, short cracks or sharp notches.

In order to overcome this drawback, several failure criteria have been proposed in the literature. Concerning numerical applications to quasi-brittle materials, we may cite the fictitious crack model (FCM) introduced by Hillerborg et al. [1], which takes into account both the tensile strength and the fracture energy of the given material. The FCM, as well as the cohesive zone model, requires a specific numerical algorithm to be inserted in structural design codes, thus providing a very versatile tool for the analysis of quasi-brittle material structures.

Anyway, easier criteria can be put forward by introducing a material length Δ, which allows one to get analytical results, at least with sufficiently simple geometries, or to couple the failure criterion with a linear elastic analysis performed through a computer simulation such as the finite element method. The task of the characteristic length Δ is to take into account the fracture toughness for the *stress based* criterion or the tensile strength for the *energy based* criterion. For the sake of clarity, we refer to the simple scheme of Fig. 1. The crack is loaded in mode *I*. It is directed along the *x*-axis and its length is 2*a*.

2. Finite fracture mechanics

We start from the stress based failure criterion (S), according to which failure is achieved when the average stress ahead of the crack tip over a Δ_S-long segment reaches the critical value σ_u. Or, equivalently, when the force resultant over a segment of length Δ_S in front of the crack tip reaches the critical value $\sigma_u \Delta_S$. This can be expressed as

$$\int_a^{a+\Delta_S} \sigma_y(x)\,\mathrm{d}x = \sigma_u \Delta_S \tag{4}$$

Obviously, this criterion provides Eq. (1) for a crack-free specimen under a tensile load. On the other hand, the value of the material length must be determined imposing Eq. (3) for a relatively large crack ($\Delta_S \ll a$). In such a case, the asymptotic stress field $\sigma_y = K_I/\sqrt{2\pi(x-a)}$ can be used; its substitution in Eq. (4) yields:

$$\Delta_S = \frac{2}{\pi}\left(\frac{K_{Ic}}{\sigma_u}\right)^2 \tag{5}$$

In order to provide meaningful results in the intermediate cases, the stress field to be inserted in Eq. (4) must be the exact one and not the asymptotic one (in the limit of $x \to a$). This means, for instance in the case of a central through-crack in an infinite body, the use of Westergaard's solution. When the exact solution is not available, the stress field can be obtained numerically by a finite element analysis.

We now turn our attention to the energy based failure criterion (E), according to which failure is achieved when the energy available during a Δ_E-long crack extension reaches the critical value $\mathscr{G}_F \Delta_E$. This can be expressed as

$$\int_a^{a+\Delta_E} \mathscr{G}(a)\,\mathrm{d}a = \mathscr{G}_F \Delta_E \quad \text{or} \quad \int_a^{a+\Delta_E} K_I^2(a)\,\mathrm{d}a = K_{Ic}^2 \Delta_E \tag{6}$$

Obviously, this criterion provides Eq. (3) for a specimen containing a large crack. On the other hand, the value of the material length must be determined imposing Eq. (1) for a vanishing crack ($a = 0$). In such a case, considering only through cracks for two-dimensional geometries, the asymptotic value for the stress-intensity
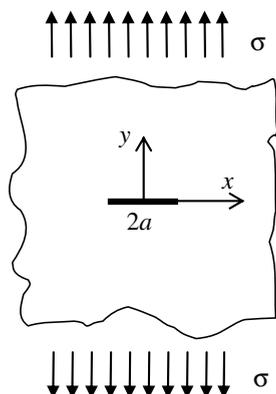

Fig. 1. Centre through crack in infinite slab under tensile load.

factor is given by $K_I = c\sigma\sqrt{\pi a}$, where c is a dimensionless factor equal to 1 for centre cracks and equal to 1.122 for edge cracks. Substituting this expression in Eq. (6) yields:

$$\Delta_E = \frac{2}{\pi} \left(\frac{K_{Ic}}{c\sigma_u} \right)^2 \tag{7}$$

In order to provide meaningful results, the function of a describing the stress-intensity factor to be inserted in Eq. (6) must be the exact one and not the asymptotic one (in the limit of $a \to 0$). Nevertheless, it is worth pointing out that, as long as the SIF vs. a functions are available in the SIF handbooks, the energy criterion (6) is much easier to apply than the stress criterion (4). In fact, the analytical solution for the stress field to be inserted in (4) is usually not available and a finite element analysis is required for *each* value of a.

A second comment on the failure criteria introduced above is that the characteristic lengths Δ (Eqs. (5) and (7)) are a measure of the material brittleness. For instance, from Eq. (4), it is clear that a very small Δ implies that only the asymptotic stress field affects the failure load: the structural behaviour is therefore brittle and governed by the material toughness (Eq. (3)). On the contrary, a very large Δ means that the failure load is affected by the whole stress field: the structural behaviour is therefore ductile and governed by the material strength (Eq. (1)).

In other words, the brittleness of the structural behaviour is provided by the ratio between the material length Δ and a length characteristic of the structure. We note that this ratio coincides with the brittleness number introduced by Carpinteri [2].

The physical meaning of the two criteria (4)–(6) is clear: fracture does not propagate continuously but by a finite crack extension, whose length is a material constant. Hence, the framework is a *finite fracture mechanics* (FFM) approach. Therefore, by definition, FFM cannot deal with continuous crack growth[1], whereas FCM can. On the other hand, from a physical point of view, it should be noted that several (perhaps all) fracture processes involve discontinuous crack growth rather than smooth, continuous growth, at least at the beginning of the cracking phenomenon (see, e.g., [3] for metals, [4] for polymers and [5] for bones). These crack jumps are likely related to material microstructure (i.e. barrier spacing or grain boundaries), giving rise to material instabilities such as snap backs. However, these microstructural processes are far from being completely understood and, in what follows, the finite extension of a crack will be assumed a priori.

Note that the crack extensions (5) and (7) for the stress and energy criteria are the same for a centre crack while slightly differ for an edge crack. The simulations performed till now [6] have shown that the predictions of the two criteria are usually close but not identical, as can be shown in some counterexamples (see, for instance, Section 5).

The stress criterion dates back to Neuber [7] and Novozhilov [8]. Afterwards, several researchers applied this criterion in a wide range of geometries and materials: see, for instance, notch analysis [9–12], fatigue problems [13] and composite materials [14].

The energy criterion as expressed by Eq. (6) was developed by Pugno and Ruoff [15], under the heading Quantized Fracture Mechanics (where its validity for nanostructures and microscopic specimens was established) and by the present authors [6], who suggested the name Finite Fracture Mechanics. These two papers have demonstrated that the approach can be used for all classes of materials, at all size scales from point defects in carbon nanotubes to large notches in engineering structures. Note that the term FFM has been already used by Hashin [16] and Kim and Nairn [17] in a different framework, i.e. the multiple cracking of coating layers and of composite laminates. In those cases, the term *finite* refers to the creation of new cracks of (although small) finite size. In spite of the different context, we decided to use the same name since the idea to substitute the infinitesimal increase of crack surface with a finite increment is the same both for our and their approach.

A slightly different form of the energy criterion (6) has been introduced by Seweryn [10]. Furthermore, a model related (but distinctly different) to FFM (sometimes called *equivalent* LEFM) involves placing a pre-existing crack at the notch root, using LEFM to predict the conditions for failure of this notch/crack

---

[1] Strictly speaking, the discrete case contains the continuous case in the limit of a vanishing increment. However, for a material with finite values of strength and toughness, FFM cannot predict a continuous crack growth.

combination. At first sight this appears similar to the present argument, but the idea breaks down if we sharpen the notch to the point at which it becomes a crack, because if a small crack is to exist at the tip of this crack then what we have is simply a longer crack so there is no reason why another small crack should not be added to it, and so on *ad infinitum*. The problem does not arise in the case of FFM since it is assumed that the crack advances discontinuously, in quanta of length Δ. Equivalent LEFM was introduced by Irwin [18] in order to take into account the plastic zone ahead of the crack tip in metals. More recently, it has been applied also to quasi brittle material failure (e.g., [19,20]). In the authors' opinion, however, the equivalent LEFM should be regarded as an approximation of the FFM approach, in the sense that equivalent LEFM can be obtained from Eq. (6) approximating the integral by the product of the middle point value times the integration interval length (i.e. $K_I^2(a + \Delta_E/2) \times \Delta_E$). It is evident that they provide the same result as far as $K_I \propto \sqrt{a}$ (e.g., the Griffith crack).

The aim of the present paper is to demonstrate some drawbacks of the FFM models (4)–(6), especially when the crack advancement is of the same order as the ligament of the specimen. We will show that coupling the energetic and stress approaches yields a new criterion which retains the advantages of previous FFM approaches and overcomes their drawbacks, since it takes into account the interaction between the finite crack extension and the geometry of the specimen. This new approach also helps to clarify the physical mechanisms underlying FFM. A fundamental result is that the finite crack extension ceases to be a material constant and becomes a structural variable.

However, before introducing the new failure criterion, it is instructive to apply the FFM criteria to the case of a Griffith crack (Fig. 1). The stress at infinity (orthogonal to the crack) is σ. We need the stress field ahead of the crack tip (Westergaard's solution) and the stress-intensity factor for any value a. By using the reference system displayed in Fig. 1, these well-known functions are, respectively:

$$\sigma_y(x) = \frac{x}{\sqrt{x^2 - a^2}} \sigma \tag{8}$$

$$K_I(a) = \sigma\sqrt{\pi a} \tag{9}$$

Substituting the expressions (8) and (9) respectively in Eqs. (4) and (6), we can obtain the failure stress σ_f, i.e. the value of the remote stress causing the crack to propagate. Interestingly the two criteria yield the same result:

$$\frac{\sigma_f}{\sigma_u} = \frac{1}{\sqrt{2(a/\Delta_S) + 1}} \tag{10}$$

observing that, in this case, $\Delta_S = \Delta_E$ because, dealing with a centre crack, $c = 1$ in Eq. (7). Eq. (10) is plotted in Fig. 2 together with the LEFM criterion (Eq. (3)), which, according to Eq. (9) provides:

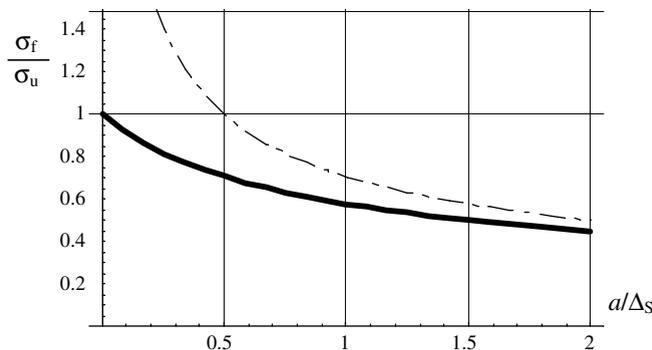$$\frac{\sigma_f}{\sigma_u} = \frac{1}{\sqrt{2(a/\Delta_S)}} \tag{11}$$

Fig. 2. Dimensionless failure stress vs. dimensionless crack length for a Griffith crack. The LEFM prediction is the dot-dashed line; the two FFM criteria (stress and energy approaches), both coincide in this particular case, giving the thick line.

The accuracy of Eq. (10) in predicting experimental data on brittle ceramic materials has been demonstrated by Taylor [21]. Note that, for a vanishing crack length, while the LEFM provides an infinite failure stress, the FFM criteria provide the required result $\sigma_f = \sigma_u$. Finally, observe that the stress and the energetic approach provide the same failure stress, but this is not always the case, as will be shown later.

3. The coupled stress and energy FFM criterion

As shown above, the classical failure criteria (1), (2) can be modified introducing an internal length, Δ, whose value is determined imposing the fulfilment of the limit cases: long crack failure load for the stress criterion and no crack failure load for the energetic criterion. Nevertheless the two approaches remain distinct and the fulfilment of one of them usually implies the violation of the other one. In other words, when applying the average stress criterion, the energy released in the crack extension is not always $\mathscr{G}_F\Delta$: hence the energy balance is violated (under the assumption that the kinetic energy associated with the dynamics of crack growth is negligible). On the other hand, when applying the energetic criterion, the resultant of the stresses acting on the crack extension can differ from the product $\sigma_u\Delta$.

In order to overcome this incongruence, we can proceed removing the hypothesis that Δ is a material constant. Note that the crack is still propagating by finite steps, i.e. we remain in the framework of FFM. The value of the finite crack extension is determined by the fulfilment of both the stress and energy criteria, i.e. when both of the following equations are satisfied:

$$\begin{cases} \int_a^{a+\Delta_{SE}} \sigma_y(x)\,\mathrm{d}x = \sigma_u\Delta_{SE} \\ \int_a^{a+\Delta_{SE}} K_I^2(a)\,\mathrm{d}a = K_{Ic}^2\Delta_{SE} \end{cases} \tag{12}$$

This means that failure takes place whenever there is a segment of length Δ_{SE} over which the stress resultant is equal to $\sigma_u\Delta_{SE}$, and, *contemporarily*, the energy available for that crack extension is equal to $\mathscr{G}_F\Delta_{SE}$. Eq. (12) represent a system of two equations in the two unknowns: σ_f, the failure load, and Δ_{SE}, the crack extension. We propose that, while each single equation represents only a *necessary* condition for failure, the fulfilment of both of them represents a necessary and *sufficient* condition for fracture to propagate. From a physical point of view, the criterion expressed in Eq. (12) is equivalent to state that *fracture is energy driven but a sufficiently high stress field must act in order to trigger crack propagation*.

The present criterion is close to the one proposed in Leguillon [22,23], where it was applied successfully to the prediction of the failure load of a three point bending beam with re-entrant corners of different amplitude. But Leguillon's formulation differs from ours because it is based on the point-wise stress criterion. To our knowledge, Eq. (12) has not been proposed in the literature yet.

Finally, observe that the application of this criterion to the Griffith crack is trivial, since, as shown in Section 2, the stress and energy approaches separately predict the same failure stress. In other words, the solution of the Eq. (12) is simply given by Eq. (10) and $\Delta_{SE} = \Delta_S = \Delta_E$. This means that the finite crack extension is constant, i.e. it is not a function of the crack length a.

4. Three point bending tests

In this section the FFM criteria (4)–(6) as well as the coupled criterion (12) are applied to the strength prediction of Three Point Bending (TPB) tests. We chose this kind of test because the stress and energy criteria provide, for small specimen sizes, strongly different results.

4.1. TPB tests of un-notched specimens

We begin by considering un-notched specimens, i.e. $a = 0$ (see Fig. 3). We assume the slenderness ratio l/b to be constant and equal to 4, l being the beam length and b its height.

As is well known, experimental data on brittle and quasi-brittle materials show an increasing strength with diminishing structural size. Therefore, the simple stress criterion (1) fails in predicting this result, whereas the FFM criteria may not.
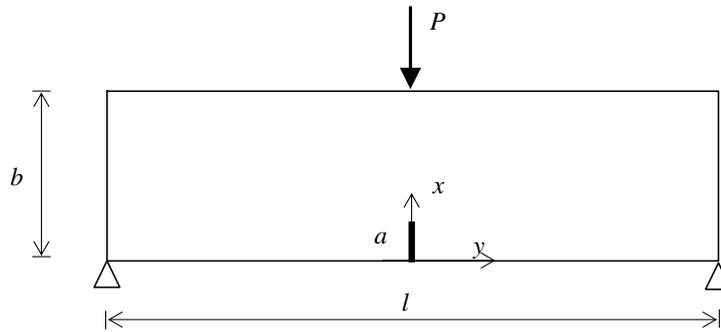
Fig. 3. Three point bending specimen.

According to simple beam theory, the stress field over the path the crack will follow, i.e. the x axis (see Fig. 3) is linear, given by

$$\sigma_y = \sigma S_0(x/b) \tag{13}$$

where $\sigma = 6P/bd$ is the maximum stress in the y direction (d being the beam thickness), reached at the bottom of the beam middle section, and S_0 is the linear function:

$$S_0(t) = 1 - 2t \tag{14}$$

Here the subscript zero refers to the value of the relative crack depth $\alpha = a/b$. Henceforth, t represents a dummy variable used for integration.

The stress-intensity factor function for cracked beams loaded in this way is not known precisely, but an analytical expression with errors less than 0.5% for any value of a is available in the stress-intensity factor handbooks:

$$K_I = \sigma\sqrt{\pi a}F(a/b) \tag{15}$$

Here function F is given by ($l/b = 4$):

$$F(t) = \frac{1}{\sqrt{\pi}}\frac{1.99 - t(1-t)(2.15 - 3.93t + 2.7t^2)}{(1+2t)(1-t)^{3/2}} \tag{16}$$

Using the stress criterion, we substitute the stress field (13) into Eq. (4). This gives:

$$\frac{\sigma_f}{\sigma_u} = \frac{\beta}{\beta - 1} \tag{17}$$

Here σ_f is the value of the maximum stress σ at failure (i.e. the apparent tensile strength) and β is the dimensionless structural size defined as the ratio between the beam height b and Δ_S. Eq. (17) is plotted in Fig. 4. It provides a failure stress σ_f equal to the tensile strength only for very large sizes. For smaller sizes, an increase of the strength is predicted, which is consistent with experimental data and with the cohesive crack model predictions [24]. On the other hand, the stress criterion predicts an infinite strength as the beam height equals Δ_S (i.e. $\beta \to 1$), since the resultant of the stresses along the whole beam ligament is zero. This result is obviously not confirmed by experiments.

To apply the energy criterion, we substitute Eq. (15) into Eq. (6), giving

$$\frac{\sigma_f}{\sigma_u} = \frac{1}{c\beta\sqrt{2\int_0^{1/\beta c^2} tF^2(t)\,dt}} \tag{18}$$

where β is defined as above for the sake of comparison with Eq. (17) and c is equal to 1.122 as prescribed by Eq. (7) when dealing with edge cracks. The integral in Eq. (18) can be solved analytically; nevertheless, for the sake of clarity, we leave it symbolically since its closed form is rather long.
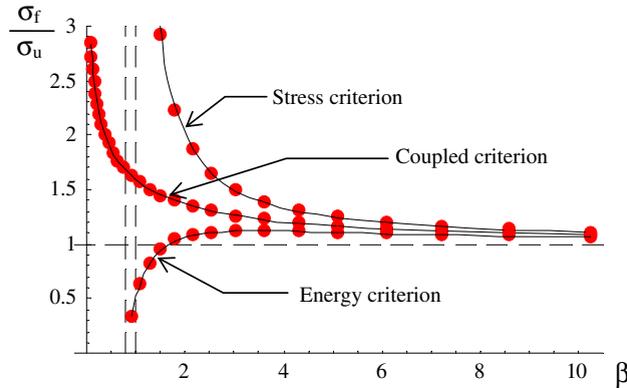
Fig. 4. Dimensionless failure stress vs. dimensionless beam size. The three curved lines represent the FFM criteria. The dashed lines represent the asymptotes.

Eq. (18) is plotted in Fig. 4. As with the stress criterion, so also the energy criterion provides a failure stress equal to the tensile strength only for very large sizes. For smaller sizes, an increase of the strength is predicted, consistent with experimental data. However, the energy criterion differs from the stress criterion in that it predicts a null strength as the beam height equals Δ_E (i.e. $\beta \to 1/c^2 = 0.794$), since the energy available at constant load is infinite in such a case. Again, this result is obviously not confirmed by experiments.

The coupled criterion (12) is able to overcome the drawbacks shown by the FFM criteria (4)–(6). Firstly, we have to substitute Eqs. (13) and (15) in the system (12). Then, in order to get an equation in a unique unknown, we can raise the second equation to the square and take the ratio side by side so as to eliminate the failure stress σ_f, giving:

$$\frac{\int_0^{\Delta_{SE}} \pi a F^2(a/b)\,\mathrm{d}a}{\left[\int_0^{\Delta_{SE}} S_0(x/b)\,\mathrm{d}x\right]^2} = \frac{K_{Ic}^2}{\sigma_u^2 \Delta_{SE}} \tag{19}$$

Introducing, as well as $\beta = b/\Delta_S$, the dimensionless variable $\varepsilon = \Delta_{SE}/b$, Eq. (19) becomes

$$2\varepsilon\beta \int_0^{\varepsilon} t F^2(t)\,\mathrm{d}t = \left[\int_0^{\varepsilon} S_0(t)\,\mathrm{d}t\right]^2 \tag{20}$$

where the unknown is the variable ε. Eq. (20) can be solved numerically: the solution changes with the value of β, the structural size. Once ε is computed, the graph of the dimensionless finite crack extension $\delta = \Delta_{SE}/\Delta_S$ vs. the dimensionless structural size β can be easily plotted (Fig. 5). The large dots represent the β values Eq. (20) is solved for; the curve is obtained by cubic spline interpolation.

Observing Fig. 5, it is seen that, for large sizes, $\delta \to 1/c^2$, i.e. Δ_{SE} tends to the constant value Δ_E. On the other hand, for small sizes, $\delta \approx \beta$, i.e. Δ_{SE} tends to cover the whole ligament b. However, the value of Δ_{SE} is always smaller than the beam ligament for any structural size. In other words, Fig. 5 shows clearly that, according to the coupled criterion (12) and differently from the FFM criteria (4)–(6), the finite crack extension is not a material constant: we can refer to it as a structural parameter, a function of material strength and toughness as well as of structural geometry and size. Interpreting it as a fracture process zone, it means that this zone scales along with the size only for small structures, while, at large sizes, it tends to a constant value. Note that this feature is shared by the cohesive crack model, since it also provides a process zone covering the whole ligament for small structural sizes [24]. On the other hand, the cohesive crack model provides a finite value for the apparent tensile strength σ_f at small sizes, in contrast with the prediction of the present criterion, as shown below.

Once ε is computed from Eq. (20), the failure stress can be deduced from one of the two Eq. (12). Choosing the first one, for the sake of simplicity, we obtain
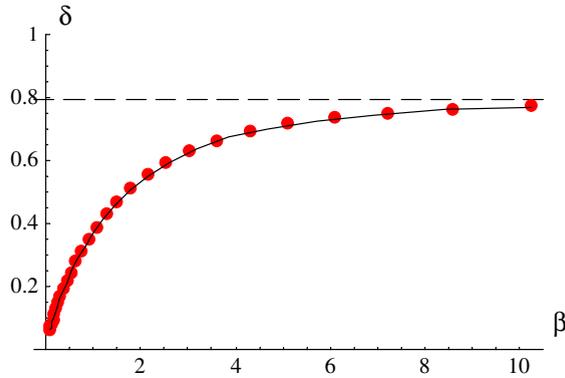
Fig. 5. Dimensionless crack extension vs. dimensionless beam height. Observe that the flat asymptote is $\delta = 1/c^2$ for large β, whereas the slant asymptote for $\beta \to 0$ is $\delta = \beta$.

$$\frac{\sigma_f}{\sigma_u} = \frac{\varepsilon}{\int_0^\varepsilon S_0(t)\, dt} = \frac{\beta}{\beta - \delta} \tag{21}$$

Eq. (21) is plotted in Fig. 4 together with Eqs. (17) and (18). They represent the size effect upon strength according to the different criteria. It is clear that all of them show the same trend for large size. On the other hand, the behaviour is very different for small specimen size. The position of the vertical asymptote changes, being at the origin only for the coupled criterion (12). Even more interesting, the same graph can be drawn in a bi-logarithmic plot (Fig. 6), where the different behaviour at small scales can be better appreciated: the coupled criterion (12) provides a straight line with a slope equal to $-1/4$. In other words, the failure stress increases with decreasing structural size as $b^{-1/4}$.

The present criterion predicts the same trend as the Multi-Fractal Scaling Law (MFSL) proposed in previous works by Carpinteri et al. [25]:

$$\sigma_f = \sigma_u \left(1 + \frac{l_{ch}}{b}\right)^{1/2} \tag{22}$$

here written according to the symbols used in the present work. l_{ch} is a material characteristic length. Both the coupled criterion (12) and the MFSL (22) provide a flat asymptote at large scales and a slant one at small scales in the bi-logarithmic plot. The following consideration can explain the main difference, i.e. the slope at small scales, equal to $1/2$ for the MFSL and to $1/4$ for the present model. The MFSL derives from a *self similar* flaw distribution (and therefore describes a *statistical* size effect, particularly suitable for materials with
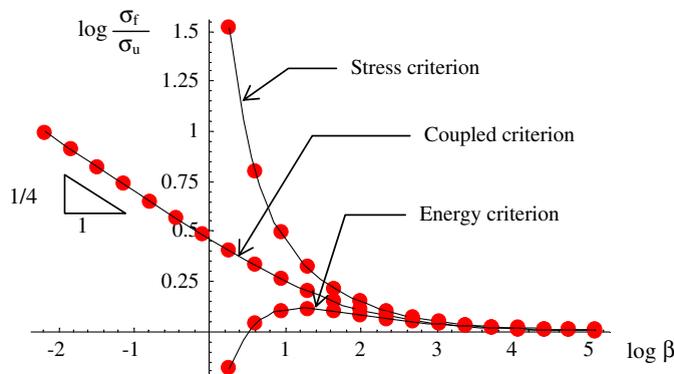

Fig. 6. Bi-logarithmic plot of failure stress vs. beam size according to FFM criteria. Only the coupled model shows a slant asymptote at small scales. Note that the strength predictions provided by the FFM coupled criterion are somehow intermediate between the ones provided by simple stress and energy FFM criteria.

heterogeneous microstructure) whereas the criterion (12) provides a size effect because of the presence of a stress gradient (a *deterministic* size effect). From this point of view, the higher slope of the MFSL at small scales is to be expected, since it includes also the effect of the flaw distribution inside the material.

Furthermore, the size effect presented here is valid only for the TPB geometry. The criterion (12) does not provide any size effect if there is no stress gradient, in the same way as the cohesive crack model. On the other hand, the scaling provided by the MFSL is much more general and able to catch the size effect, experimentally verified, in direct tension tests, i.e. when the stress distribution over the ligament is uniform.

4.2. TPB tests of notched specimens

By a further effort, the coupled criterion (12) can be applied also to the strength prediction of notched TPB specimens. The main difficulty is due to the fact that only the asymptotic stress field in front of the crack tip is known analytically, whereas we require the whole stress field along the ligament. Therefore we performed a finite element analysis for a range of relative crack depths $\alpha = a/b$ and obtained the stress function S_α by interpolation. The subscript α reminds us that the stress function changes with α:

$$\sigma_y = \sigma S_\alpha(x/b) \tag{23}$$

Note that now $x = 0$ corresponds to the crack tip. Proceeding as in the previous section, we obtain the following equation in the unknown ε:

$$2\varepsilon\beta \int_\alpha^{\alpha+\varepsilon} tF^2(t)\,dt = \left[\int_0^\varepsilon S_\alpha(t)\,dt \right]^2 \tag{24}$$

Note that Eq. (24) is a generalization of Eq. (20), since it can be obtained by letting $\alpha = 0$ in Eq. (24). Fixing the two parameters α and β, ε can be computed. Hence, the failure stress can be deduced from the first equation of the system (12) as follows:

$$\frac{\sigma_f}{\sigma_u} = \frac{\varepsilon}{\int_0^\varepsilon S_\alpha(t)\,dt} \tag{25}$$

The results are plotted in the bi-logarithmic graph of Fig. 7, where the dimensionless strength vs. the dimensionless size is drawn for different values of the relative crack depth. It is seen that, at small sizes, all the curves show the same slope 1/4 valid for un-notched structures. On the other hand the behaviour at large size is
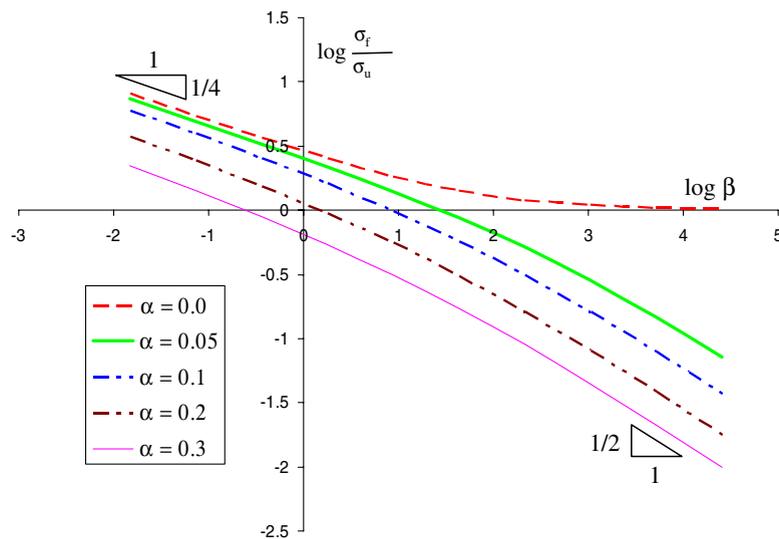
Fig. 7. Bi-logarithmic plot of failure stress vs. specimen size for various relative crack depths. Note that the slope is equal to 1/4 at small scales and 0 or 1/2 at large scales.

completely different: the un-notched structure strength tends to a constant value (the tensile strength σ_u) whereas the notched structure strength decreases with the 1/2 LEFM slope. For the sake of clarity, in Fig. 7 we did not draw the predictions based upon the FFM criteria (4)–(6), since they provide the same drawbacks shown above for un-notched specimens.

Observing Fig. 7, it is interesting to point out that the coupled criterion (12) is able to catch the concave–convex transition when passing from notched to un-notched specimens in the log-log plot. While for the notched structures the slope increases from 1/4 to 1/2 (in absolute value), for the un-notched structures it decreases from 1/4 to 0.

A comparison can be made between this analysis and the Size Effect Law (SEL) proposed by Bažant [26]:

$$\sigma_f = \sigma_0 \left(1 + \frac{b}{b_0}\right)^{-1/2} \tag{26}$$

here written according to the symbols used in the present work: b_0 is the so-called transitional size and σ_0 the strength for vanishing size of a given geometry. The comparison is allowable because, differently from the MFSL, both the present approach and the SEL do not take into account the statistical flaw size distribution inside material microstructure: therefore, they are not able to predict any size effect if there is no stress gradient. In other words, they deal only with the deterministic size effect.

The main difference is in the small scale behaviour. Unlike the present approach, because of different assumptions in the two models, the SEL provides a constant value (once the relative crack depth is fixed) for vanishing structural size. On the other side, the large scale behaviour is substantially the same. This result should have been expected since the SEL was firstly derived by truncating the Taylor expansion of the equivalent LEFM criterion – the point-wise counterpart of Eq. (6) – at large scales. On the other hand, at the same scales, the present approach coincides with the energy criterion (6), since Δ tends to the constant value (7), as shown in Fig. 5.

5. Comparison with experimental data

In order to have a feedback for the proposed model, we present a comparison with the data obtained by Karihaloo [27]. He tested TPB high strength concrete specimens of various sizes and with different relative crack depths. The slenderness l/b and the thickness d were kept constant and equal respectively to 4 and 10 cm.
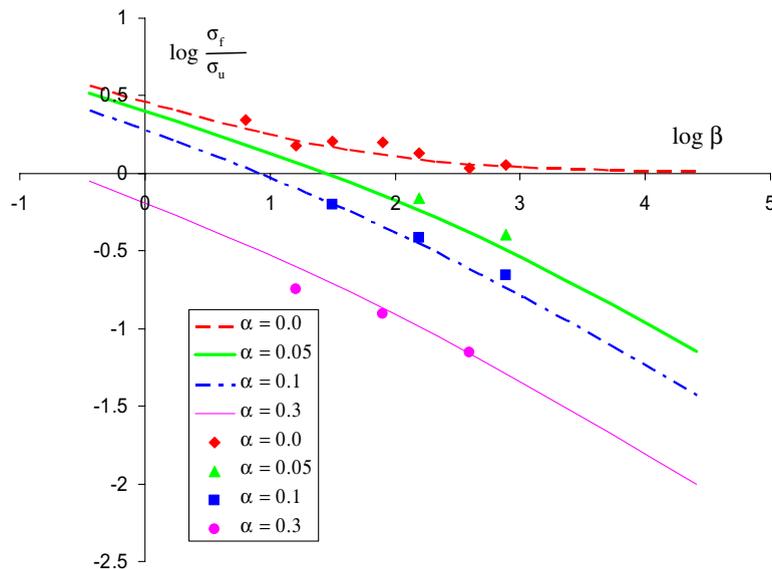

Fig. 8. Bi-logarithmic plot of failure stress vs. specimen size for various relative crack depths: comparison with experimental data on high strength concrete specimens obtained by Karihaloo [27].

His data are plotted in Fig. 8 together with the predictions of the coupled FFM model. The values of the tensile strength and of the fracture toughness were determined by a best fit procedure: we found 8.27 MPa for strength and 1.52 MPa$\sqrt{m}$ for toughness. As expected, these values are a lower bound among the *apparent* tensile strengths of un-notched specimens (8.28 MPa being the minimum value) and an upper bound for the *apparent* fracture toughness of notched specimens (1.48 MPa$\sqrt{m}$ being its maximum value).

It can be seen from Fig. 8 that the predictive accuracy of the coupled criterion is very good. In the paper by Karihaloo [27], the same data are fitted using the MFSL, the SEL and a general law proposed by Karihaloo himself. A great advantage of the present approach is that only two parameters are needed to fit all the data, whereas the parameters of the other laws have to be determined for *each* relative crack depth. Furthermore, while the parameters of the SEL as well as the ones of the MFSL are mainly empirical constants, the two best fit parameters of the present criterion show a clear physical meaning, being the tensile strength and the fracture toughness. This feature is shared by the cohesive crack model (see, for a review, [28]), which, however, requires a specific computer code in order to be implemented. As a drawback, it should be highlighted that the results presented herein are restricted to the TPB geometry. Applications to other shapes would require suitable solutions of the system (12), which can be obtained either analytically or numerically. Further comparisons are also needed in order to validate the present approach.

Finally, it is interesting to observe that, analysing only the data relative to the un-notched specimens and using the coupled criterion (in this case, Eqs. (20) and (21)), the best fit procedure provides a fracture toughness equal to 1.50 MPa$\sqrt{m}$. This value is very close to the one obtained applying LEFM to the large notched specimens (1.48 MPa$\sqrt{m}$). In other words, the method presented herein is able to provide the fracture toughness using test data from un-notched specimens, as long as the range of specimen sizes is broad enough. This implies that the mechanism of fracture is the same, whether or not a pre-crack is present.

6. Conclusions

In the present paper, we introduced a new failure criterion. It was obtained by coupling the stress and energy finite fracture mechanics approaches and allowing the finite crack extensions to vary according to the specific geometry and loading.

A preliminary discussion of the two starting criteria has been provided. The stress method is a well-known criterion. On the other hand, the energy approach has been introduced more recently: it relies on the assumption of a crack growth by finite steps. However, using a constant value for the interval over which the stress is averaged or for the crack advance, means that one of the two criteria will be violated.

On the other hand, removing the hypothesis of a constant crack advance, it is possible to formulate a coupled FFM criterion that is consistent with both the energetic and stress criteria. In order to check its soundness, we performed a comparison with experimental data on high strength concrete three point bending specimens of different sizes. We showed that the coupled model is able to catch the size effect in quasi brittle material structures and, particularly, the concave–convex transition in the bi-logarithmic plot when passing from un-notched to notched specimens. Furthermore, for the sake of completeness, we provided a brief comparison with general size effect laws available in the literature.

We believe that the different FFM theories reviewed in the present paper (stress, energy, coupled criterion as well as their point-wise counterparts), which are based on the presence of an internal length, should be relevant to different mechanisms of failure. As a consequence, the most suitable fracture criterion could change from case to case. Further efforts are therefore required to link these theories to the real failure mechanisms.

References

[1] Hillerborg A, Modéer M, Petersson PE. Analysis of crack formation and crack growth in concrete by means of fracture mechanics and finite elements. Cem Concr Res 1976;6:773–82.
[2] Carpinteri A. Static and energetic fracture parameters for rocks and concretes. Mater Struct (RILEM) 1981;14:151–62.
[3] Blom A, Hedlund A, Zhao W, Fathulla A, Weiss B, Stickler R. Short fatigue crack growth behaviour in Al2024 and Al7475. In: Miller KJ, de los Rios ER, editors. The behaviour of short fatigue cracks. London: MEP; 1986. p. 36–66.
[4] Kinloch AJ, Shaw SJ, Tod DA, Hunston DL. Deformation and fracture behaviour of a rubber-toughened epoxy: 1. Microstructure and fracture studies. Polymer 1983;24:1341–54.

[5] Hazenberg JG, Taylor D, Lee TC. Mechanisms of short crack growth at constant stress in bone. J Biomech 2006;27:2114–22.

[6] Taylor D, Cornetti P, Pugno N. The fracture mechanics of finite crack extension. Engng Fract Mech 2005;72:1021–38.

[7] Neuber H. Theory of notch stresses. Berlin: Springer; 1958.

[8] Novozhilov V. On a necessary and sufficient condition for brittle strength. Prik Mat Mek 1969;33:212–22.

[9] Sih GC. Mechanics of fracture initiation and propagation: surface and volume energy density applied as failure criterion. Dordrecht: Kluwer; 1991.

[10] Seweryn A. A non-local stress and strain energy release rate mixed mode fracture initiation and propagation criteria. Engng Fract Mech 1998;59:737–60.

[11] Taylor D, Merlo M, Pegley R, Cavatorta MP. The effect of stress concentrations on the fracture strength of polymethylmethacrylate. Mater Sci Engng A 2004;382:288–94.

[12] Carpinteri A, Pugno N. Fracture instability and limit strength conditions in structures with re-entrant corners. Engng Fract Mech 2005;72:1254–67.

[13] Taylor D. Geometrical effects in fatigue: a unifying theoretical model. Int J Fatigue 1999;21:413–20.

[14] Whitney JM, Nuismer RJ. Stress fracture criteria for laminated composites containing stress concentrations. J Compos Mater 1974;8:253–65.

[15] Pugno N, Ruoff N. Quantized fracture mechanics. Philos Mag A 2004(84/27):2829–45.

[16] Hashin Z. Finite thermoelastic fracture criterion with application to laminate cracking analysis. J Mech Phys Solids 1996;44:1129–45.

[17] Kim SR, Nairn JA. Fracture mechanics analysis of coating/substrate systems. Part I: Analysis of tensile and bending experiments. Engng Fract Mech 2000;65:573–93.

[18] Irwin GR. Analysis of stresses and strains near the end of a crack traversing a plate. J Appl Mech 1957;24:361–4.

[19] Karihaloo B. Fracture mechanics and structural concrete. Harlow: Longman; 1995.

[20] Bažant ZP. Scaling of structural strength. London: Hermes Penton Science; 2002.

[21] Taylor D. Predicting the fracture strength of ceramic materials using the theory of critical distances. Engng Fract Mech 2004;71:2407–16.

[22] Leguillon D. Strength or toughness? A criterion for crack onset at a notch. Europ J Mech A/Solids 2002;21:61–72.

[23] Leguillon D, Yosibash Z. Crack onset at a v-notch. Influence of the notch tip radius. Int J Fract 2003;122:1–21.

[24] Carpinteri A. Decrease of apparent tensile and bending strength with specimen size: two different explanations based on fracture mechanics. Int J Solids Struct 1989;25:407–29.

[25] Carpinteri A, Chiaia B, Ferro G. Size effects on nominal tensile strength of concrete structures: multifractality of material ligaments and dimensional transition from order to disorder. Mater Struct (RILEM) 1995;28:311–7.

[26] Bažant ZP. Size effect in blunt fracture: concrete, rock, metal. ASCE J Engrg Mech 1984;110:518–35.

[27] Karihaloo BL, Abdalla HM, Xiao QZ. Size effect in concrete beams. Engng Fract Mech 2003;70:979–93.

[28] Carpinteri A, Cornetti P, Barpi F, Valente S. Cohesive crack model description of ductile to brittle size-scale transition: dimensional analysis vs. renormalization group theory. Engng Fract Mech 2003;70:1809–39.